On estimating the amplitude of harmonic vibration from the Doppler spectrum of reflected signals

Sung-Rung Huang
Department of Electrical Engineering, University of Rochester, Rochester, New York 14627

Robert M. Lerner
Department of Radiology, University of Rochester, Rochester, New York 14642

Kevin J. Parker
Rochester Center for Biomedical Ultrasound, University of Rochester, Rochester, New York 14627

(Received 8 May 1990; accepted for publication 6 August 1990)

The Doppler spectrum of echoes from a sinusoidally vibrating scatterer has discrete spectral lines weighted by Bessel functions of the first kind. Because the signal and spectrum are complicated functions of the vibration amplitude, a number of different approaches have been tried in the past to estimate the vibration amplitude, given a received signal. Here, a new and simple relationship between the spread (or variance) of the Doppler spectrum and the vibration amplitude is derived. A method of estimating the vibration amplitude is proposed based on this relation and a noise compensation procedure is also demonstrated. The performance of the estimators is studied through simulations. High accuracy is predicted under proper sampling conditions even when the signal-to-noise ratio is poor. Slight deviations from single-frequency oscillation, as would be caused by nonlinear or nonideal medium or source effects, are found to have little contribution to the total estimation error.

PACS numbers: 43.60.Gk, 43.20.Fn, 43.30.Es

INTRODUCTION

The general problem of Doppler shifts from objects with time-varying velocity in an inhomogeneous or layered medium is quite complex. It is still a subject of controversy involving linear and nonlinear derivations.[1,2] However, when the scattering object is vibrating slowly so as to produce a wavelength much larger than the geometrical dimensions of the scatterer itself, the Doppler spectrum of the signals returning from sinusoidally oscillating structures is similar to that of a pure-tone frequency modulation (FM) process.[3] This spectrum is a Fourier series with spectral lines lying above and below the carrier frequency. The spacing between spectral harmonics is equal to the vibration frequency, and the amplitudes of harmonics are given by different orders of Bessel functions of the first kind.[3] A number of applications in acoustics, optics, and radio have led to research on extracting the vibration parameters from a measured Doppler spectrum. Amplitude, phase, and frequency of the oscillating structure are the most typical parameters to be estimated.

Many techniques have been proposed to estimate the vibrational parameters. Holen *et al.*[4] measured the vibration frequency of oscillating heart valves by looking visually at the spacing between harmonics in the ultrasound Doppler spectrogram. The vibration amplitude is estimated by counting the number of significant harmonics under a certain threshold. This procedure is relatively coarse but is related to the observation in FM that the bandwidth is roughly proportional to the modulation parameter, or amplitude of oscillation.[3] Taylor[5,6] studied the laser calibration of microphones, and determined the vibration amplitude by fitting the theoretical spectrum with an unweighted least-squares approximation. Lerner *et al.*[7] in their new technique for medical imaging of elastic properties of tissue called "sonoelasticity imaging," have suggested the estimation of vibration amplitude by calculating the ratio of the two largest harmonics. Jarzynski *et al.*[8] undertake a similar estimation for precision measurement of the sound fields with laser Doppler by comparing the ratio of carrier and fundamental harmonics. Similar estimation had also been made by Cox and Rogers[9] to study the vibrational motion of auditory organs in fish. Observing that the ratios of the adjacent Bessel coefficients increase monotonically, Yamakoshi *et al.*[10] came up with an estimator by comparing the relative magnitude of the adjacent harmonics in their study of tissue motion. They also derive the vibration phase from the fundamental spectral components of two quadrature channels. All of these techniques can be broadly classified in the same category, or approach to estimation of the vibrational parameters using some ratio of amplitudes. One of the disadvantages of the ratio methods is that they require either intensive computation or large look-up tables of theoretical Bessel functions for comparison with the measured data. Besides, ratio methods work well only when the argument of the Bessel function is small, which poses a severe limitation on the range of estimation. Furthermore, in practice, the performance of the ratio methods is highly degraded since almost all Doppler spectra suffer from poor signal-to-noise ratio.

Finally, a sophisticated algorithm is required to determine the best selection of the harmonic pair to be compared.

 0001-4966/90/122702-11$00.80

Therefore, this work presents a simple and noise-immune algorithm for vibration estimation.

The problem of vibration amplitude estimation is approached through the measurement of the spectral spread (or variance) of the Doppler spectrum. The proposed estimation techniques can be implemented without difficulties. For instance, in clinical applications of Doppler ultrasound, one could obtain the necessary parameters with slight modifications of existing instruments. Significant improvement on estimation accuracy can be further achieved with a noise correction algorithm. The theoretical derivations of the estimation and results of simulation are shown in the following section. The effects of noise, sampling, and nonlinearity on the estimator performance are also demonstrated subsequently.

I. THEORY

A. Derivation of the Doppler spectrum

Since the FM spectrum is well known, we briefly summarize results in this section and introduce our notation. When a moving object is illuminated with an incident laser, radio, or acoustic wave, the detected backscattered signals from that moving object will demonstrate a frequency shift known as the Doppler shift. If the scatterer is oscillating with the vibration velocity much slower than the wave speed and the vibration frequency much less than the carrier (incident wave) frequency, the spectrum of the detected scattered wave will be similar to that of a pure-tone FM process since the instantaneous frequency of the scattered waves has a Doppler shift proportional to the vibration velocity. Assume that the transmitted or incident signal is

$$s_t(t) = \cos(\omega_0 t), \tag{1}$$

and the scatterers are vibrating with the form

$$\xi(t) = \xi_m \sin(\omega_L t + \varphi), \tag{2}$$

$$v(t) = \dot{\xi}(t) = v_m \cos(\omega_L t + \varphi), \tag{3}$$

where $\xi(t)$ is the displacement of the vibration, $v(t)$ is the velocity of the vibration, ω_L is the vibration frequency, φ is the vibration phase, ξ_m is the vibration amplitude of the displacement field, and $v_m = \omega_L \xi_m$ is the vibration amplitude of the velocity field.

The instantaneous frequency of the received or scattered waves will be shifted to

$$\omega_i = \omega_0 + \Delta\omega_d, \tag{4}$$

$$\Delta\omega_d = \Delta\omega_m \cos(\omega_L t + \varphi), \tag{5}$$

$$\Delta\omega_m = 2v_m\omega_0 \cos\theta / c_0, \tag{6}$$

where ω_i is the instantaneous frequency of the scattered waves, $\Delta\omega_d$ is the Doppler shift, c_0 is the propagation speed of illuminating wave at frequency ω_0, and θ is the angle between the wave propagation and the vibration vectors.

Therefore, the received or scattered waves can be written as

$$s_r(t) = A \cos[\omega_0 t + (\Delta\omega_m/\omega_L)\sin(\omega_L t + \varphi)] \tag{7}$$

since the instantaneous frequency is, by definition, given by the time derivative of the argument of the carrier cosine wave.

Using trigonometric identities, Eq. (7) can be replaced by the series[3]

$$s_r(t) = A \sum_{n=-\infty}^{\infty} J_n(\beta)\cos[\omega_0 t + n(\omega_L t + \varphi)], \tag{8}$$

where the modulation index or the argument of the Bessel functions β is directly related to the vibration amplitude of the velocity or displacement field as follows:

$$\beta \equiv \frac{\Delta\omega_m}{\omega_L} = \frac{2v_m\omega_0 \cos\theta}{\omega_L c_0} = \frac{2\xi_m\omega_0 \cos\theta}{c_0} = 4\pi\frac{\xi_m}{\lambda_0}\cos\theta, \tag{9}$$

where λ_0 is the wavelength associated with the wave of frequency ω_0 and propagation speed c_0.

Thus, given the Doppler spectrum as described above, the estimation of the vibration amplitude is equivalent to the estimation of the Bessel argument β. The exact spectral shape of the Doppler signal is complicated and dependent on the parameter β. Examples of Doppler spectra from low, medium, and high values of β and the two quadrature components of the corresponding Doppler signal are given in Figs. 1 and 2, respectively. Given a measured spectrum, it can be seen that the backward estimation of β is not straightforward, even in the noise-free case. Experimental time-frequency display data from an ultrasound B-scan instrument with Doppler capabilities are given in Fig. 3. The vibration frequency is fixed, while the vibration amplitude, which is proportional to the parameter β, is increased from left to right, then decreased. More sidebands plus aliasing show up when the parameter β increases. As shown in Fig. 2, the two quadrature components of the Doppler signal corresponding to those in Fig. 1 are also complex. Thus a time domain estimation approach is not obvious. The estimation is even more difficult when the background noise is mixed with the signal, as shown in Fig. 4.

B. Vibration estimation from Doppler spectral spread

Two Doppler spectral parameters, spectral variance (or spectral spread) and mean Doppler frequency, are usually defined as:

$$\sigma_\omega^2 = \int_{-\infty}^{\infty} (\omega - \overline{\omega})^2 S(\omega)d\omega \left(\int_{-\infty}^{\infty} S(\omega)d\omega\right)^{-1} \tag{10}$$

and

$$\overline{\omega} = \int_{-\infty}^{\infty} \omega S(\omega)d\omega \left(\int_{-\infty}^{\infty} S(\omega)d\omega\right)^{-1}, \tag{11}$$

where σ_ω is the Doppler spectral spread (σ_ω^2 is the variance or second moment), $\overline{\omega}$ is the mean frequency shift of the Doppler spectrum (the first moment), and $S(\omega)$ is the Doppler power spectrum downshifted to baseband. Note that the mean Doppler frequency shift $\overline{\omega}$ is not necessarily zero since the Doppler signal is generally complex and the Doppler spectrum $S(\omega)$ can be asymmetric.

If the scatterer is vibrating, the Doppler power spectrum that can be derived from Eq. (8) in the previous section is

$$S(\omega) = 2\pi \sum_{n=-\infty}^{\infty} J_n^2(\beta)\delta(\omega - n\omega_L), \tag{12}$$

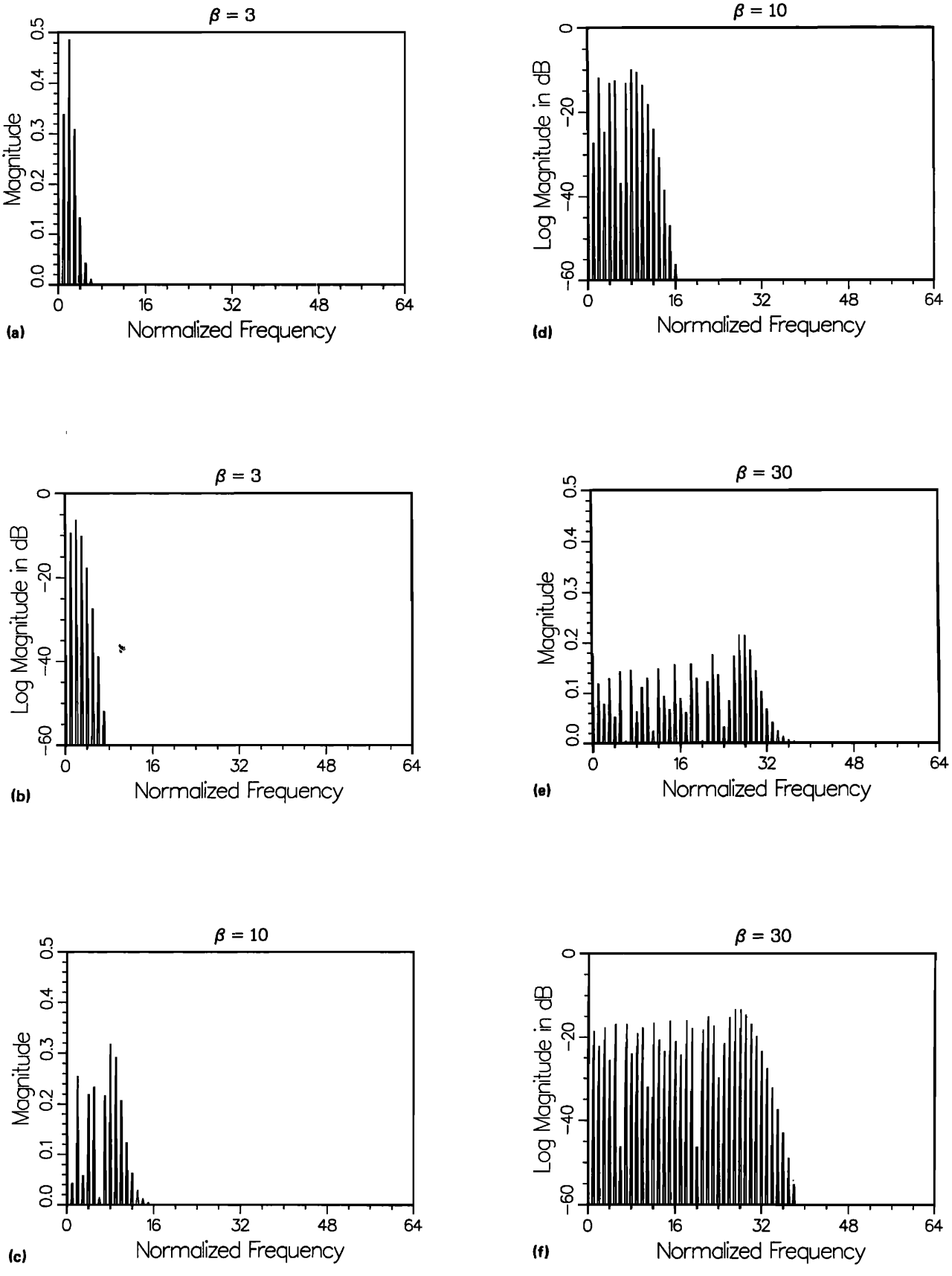

FIG. 1. Examples of noise-free Doppler spectra for low $\beta = 3$: (a) linear and (b) log scale; medium $\beta = 10$: (c) linear and (d) log scale; high $\beta = 30$: (e) linear and (f) log scale. Normalized fold-over frequency $f_{\text{fold}} = 64$, normalized segment length $T_{\text{FFT}} = 4$, for all cases.

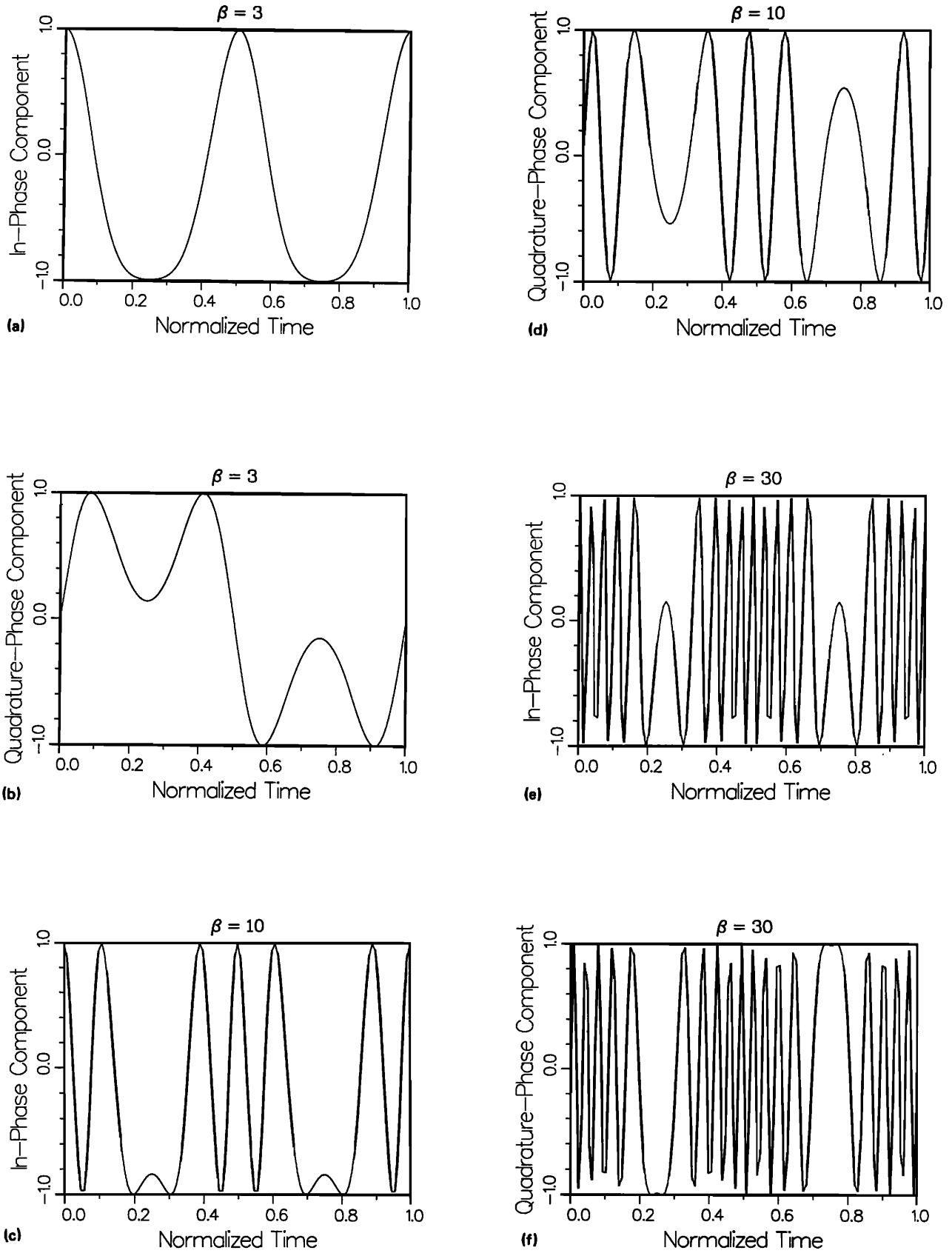

FIG. 2. Examples of two quadrature components of noise-free Doppler signals for low $\beta = 3$: (a) in-phase and (b) quadrature-phase component; medium $\beta = 10$: (c) in-phase and (d) quadrature-phase component; high $\beta = 30$: (e) in-phase and (f) quadrature-phase component. Since the function is periodic, only one cycle is shown in the graphs.

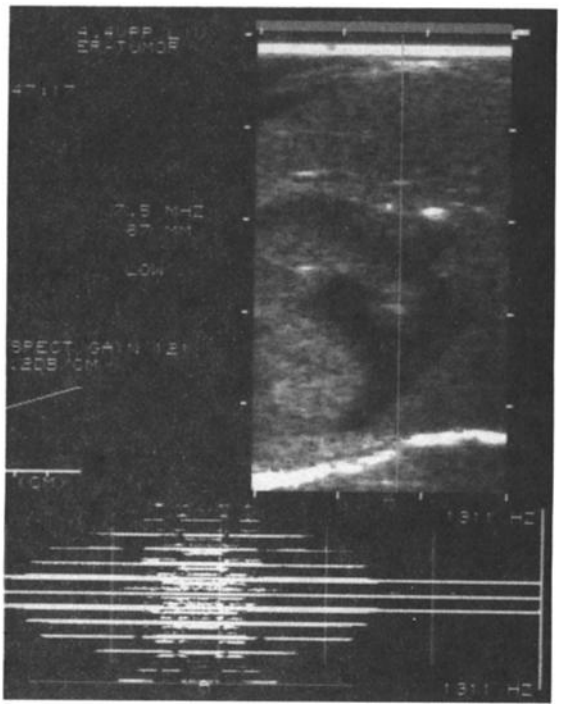

FIG. 3. Experimental observation of Doppler spectrum from vibrating structures under clinical *B*-scan ultrasound. The lower portion is a time (horizontal)-frequency (vertical) display of data from the region selected by the cursor as shown on the upper portion. Vibration frequency is held fixed, while vibration amplitude is increased and then decreased from left to right.

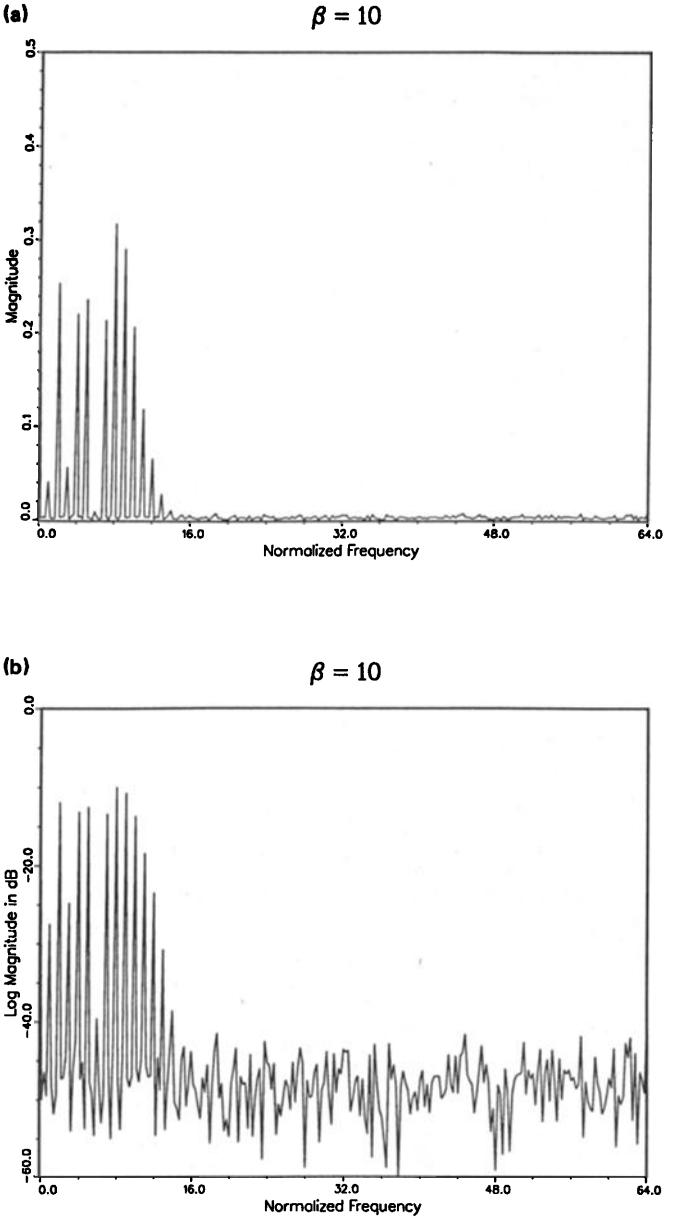

FIG. 4. Example of noisy Doppler spectrum with $\beta = 10$, signal-to-noise ratio SNR = 20 dB, normalized fold-over frequency $f_{\text{fold}} = 64$, and normalized segment length $T_{\text{FFT}} = 4$, (a) linear scale, (b) log scale.

where the power spectrum has been downshifted to zero frequency, as by quadrature detection.

For this particular Bessel spectrum, the mean frequency $\bar{\omega}$ is zero since $J_{-n}(\beta) = (-1)^n J_n(\beta)$ and the power spectrum is therefore symmetric about zero frequency. Thus, the spectral spread can be calculated from the zeroth and second moments of the spectrum defined as

$$m_0 = \sum_{n=-\infty}^{\infty} J_n^2(\beta), \tag{13}$$

$$m_2 = \sum_{n=-\infty}^{\infty} (n\omega_L)^2 J_n^2(\beta), \tag{14}$$

where m_k is the k th moment of the Doppler spectrum.

However, the zeroth moment is the total energy of the signal and is equal to unity. One can easily show this using the following mathematical identity:

$$e^{i\beta \sin\theta} = \sum_{n=-\infty}^{\infty} J_n(\beta) e^{in\theta}. \tag{15}$$

Squaring the above equation and replacing θ with $-\theta$ in one term, we have

$$1 = e^{i\beta \sin\theta} e^{i\beta \sin(-\theta)}$$

$$= \sum_{m=-\infty}^{\infty} \sum_{n=-\infty}^{\infty} J_m(\beta) J_n(\beta) e^{i(m-n)\theta}. \tag{16}$$

Integrating the above equation over one period ($\theta = 0$ to 2π), and using orthogonality of exponential functions for $m \neq n$,

$$1 = \sum_{n=-\infty}^{\infty} J_n^2(\beta) = m_0, \tag{17}$$

a result that has been noted in the literature.[11]

The second moment can be derived in the same way by taking the first derivative of the Eq. (15) with respect to θ,

$$\beta \cos\theta e^{i\beta \sin\theta} = \sum_{n=-\infty}^{\infty} n J_n(\beta) e^{in\theta}. \tag{18}$$

Squaring from the above equation as before,

$$\beta^2 \cos^2\theta e^{i\beta\sin\theta} e^{i\beta\sin(-\theta)}$$

$$= \sum_{m=-\infty}^{\infty} \sum_{n=-\infty}^{\infty} mn J_m(\beta) J_n(\beta) e^{i(m-n)\theta}. \quad (19)$$

Then, integrating over one period again,

$$\frac{\beta^2}{2} = \sum_{n=-\infty}^{\infty} n^2 J_n^2(\beta) = m_2. \quad (20)$$

In general, all moments of the Bessel spectrum can be calculated from derivatives of Eq. (15) by proper differentiation, squaring, and integration. Low-order moments of the Bessel spectrum are given in Table I.

These moments of the Bessel spectrum can also be calculated from the generating function of Bessel function:

$$\mathcal{J}(\beta,z) \equiv \sum_{n=-\infty}^{\infty} z^n J_n(\beta) = e^{(\beta/2)[z-(1/z)]}, \quad (21)$$

which can be found in a standard handbook on bessel functions.[11] By taking the 1st through the k th derivative of the generating function with respect to z and substituting $z=1$ into the resulting expressions, all moments of the Bessel spectrum, as functions of the parameter β, can then be calculated from lower-order moments by squaring and simple algebraic manipulation.

From this point of view, the Bessel spectrum is actually a one-parameter function. Therefore, the second moment serves as a good estimator of the spectrum.

One can estimate the vibration from the Doppler spectral spread as

$$\sigma_\omega^2 = (m_2 - m_1^2)/m_0 = [m_2 - (\overline{\omega})^2]/m_0, \quad (22)$$

and for this case of the Doppler spectrum, $\overline{\omega} = 0$, thus

$$\sigma_\omega^2 = \sum_{n=-\infty}^{\infty} (n\omega_L)^2 J_n^2(\beta) \left(\sum_{n=-\infty}^{\infty} J_n^2(\beta) \right)^{-1}, \quad (23)$$

or

$$\beta = \sqrt{2}(\sigma_\omega/\omega_L). \quad (24)$$

This indicates that the amplitude parameter β can be estimated from the standard deviation of the power spectrum. This straightforward result has, apparently not been previously derived for the case of FM broadcast or Doppler spectrum from vibrating objects.

C. Noise correction algorithm

In practical situations, noise presents problems in parameter estimation. The Doppler signals tend to be 30–50 dB lower than the carrier in many applications, therefore, the signal-to-noise ratio for Doppler signal is usually poor. Additive, stationary, and uncorrelated noise can be removed from the Doppler spectral spread vibration estimator. If stationary uncorrelated noise with power spectrum $N(\omega)$ is added in the received backscattered signal, the noisy Doppler spectral spread σ_ω can be written as

$$\sigma_\omega^2 = \int_{-\infty}^{\infty} (\omega - \overline{\omega})^2 \left(\sum_{n=-\infty}^{\infty} J_n^2(\beta)\delta(\omega - n\omega_L) + N(\omega) \right) d\omega \times \left[\int_{-\infty}^{\infty} \left(\sum_{n=-\infty}^{\infty} J_n^2(\beta)\delta(\omega - n\omega_L) + N(\omega) \right) d\omega \right]^{-1}$$

$$= (m_{2,S} + m_{2,N})/(m_{0,S} + m_{0,N})$$

$$= [\sigma_{\omega,S}^2 + (1/\mathrm{SNR})\sigma_{\omega,N}^2]/[1 + (1/\mathrm{SNR})], \quad (25)$$

where $\overline{\omega}$ is the mean Doppler shift of the noisy signal given by

$$\overline{\omega} = \int_{-\infty}^{\infty} \omega \left(\sum_{n=-\infty}^{\infty} J_n^2(\beta)\delta(\omega - n\omega_L) + N(\omega) \right) d\omega \times \left[\int_{-\infty}^{\infty} \left(\sum_{n=-\infty}^{\infty} J_n^2(\beta)\delta(\omega - n\omega_L) + N(\omega) \right) d\omega \right]^{-1}, \quad (26)$$

$m_{k,S}$ and $m_{k,N}$ are the k th moment of signal and noise about the corresponding mean frequencies respectively, $\sigma_{\omega,S}$ is the Doppler spectral spread of vibration only, $\sigma_{\omega,N}$ is the Doppler spectral spread of noise only, and SNR is the signal-to-noise ratio given by

$$\mathrm{SNR} = \int_{-\infty}^{\infty} \left(\sum_{n=-\infty}^{\infty} J_n^2(\beta)\delta(\omega - n\omega_L) \right) d\omega \times \left(\int_{-\infty}^{\infty} N(\omega) d\omega \right)^{-1}$$

$$= m_{0,S}/m_{0,N} = 1/m_{0,N}. \quad (27)$$

As long as the noise is stationary, the moments of noise power spectrum can be estimated when the vibration is removed or halted. Once the noise moments have been estimated, the noise-free vibrational Doppler spectral spread can then be estimated from the noisy signal as

$$\sigma_{\omega,S}^2 = \sigma_\omega^2 [1 + (1/\mathrm{SNR})] - (1/\mathrm{SNR})\sigma_{\omega,N}^2. \quad (28)$$

In some applications, the vibration is inherent and cannot be controlled externally. The noise compensation, in this case, can be done by estimating the signal-to-noise ratio as well as the Doppler spectral spread of the noise from the finite bandwidth white noise assumption as follows:

$$m_{0,N} = \int_{-B}^{B} N_0 \, d\omega = 2N_0 B, \quad (29)$$

$$m_{2,N} = \int_{-B}^{B} \omega^2 N_0 \, d\omega = \frac{2N_0 B^3}{3}, \quad (30)$$

$$\sigma_{\omega,N}^2 = (2N_0 B^3/3)/2N_0 B = B^2/3, \quad (31)$$

where N_0 is the power spectral density of the white noise, and B is the one-sided bandwidth of the white noise.

TABLE I. Low-order moments of the Bessel spectrum.

All odd moments	0
0th moment	1
2nd moment	$\frac{1}{2}\beta^2$
4th moment	$\frac{1}{2}\beta^2 + \frac{3}{8}\beta^4$
6th moment	$\frac{1}{2}\beta^2 + \frac{15}{8}\beta^4 + \frac{5}{16}\beta^6$

Even when the noise is not white, the noise compensation is still possible as long as noise power and noise spectral spread can be estimated *a priori* by statistical techniques.

II. RESULTS AND DISCUSSIONS

Simulated Doppler spectra are obtained by taking fast Fourier transform (FFT) of finite segments that are composed of the two quadrature components of Eq. (7). Figures 5–9 are families of the estimation errors $[(\hat{\beta}-\beta)/\beta]\times 100\%$ as functions of various parameters in the estimation process, where $\hat{\beta}$ is the estimated vibration parameter and β is the true parameter.

A. Effects of noise

The estimation errors are plotted as functions of signal-to-noise ratio from 0–40 dB in Fig. 5(a). White Gaussian noise was added independently into the two quadrature components. The normalized sampling frequency (defined as sampling frequency divided by the vibration frequency) is 128. Or equivalently, the normalized fold-over frequency (defined as fold-over frequency, or aliasing frequency, or half-sampling frequency divided by the vibration frequency) is 64. A high sampling rate was used to reduce the aliasing

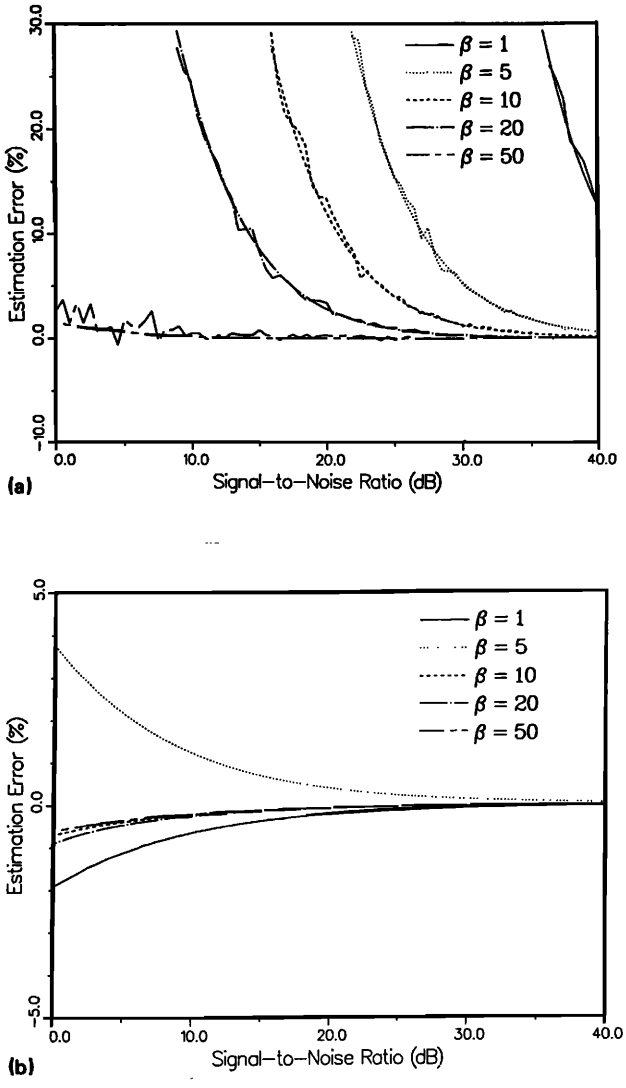

FIG. 5. Plot of estimation errors in percentage against signal-to-noise ratio from 0–40 dB at normalized fold-over frequency $f_{\text{fold}} = 64$ and normalized segment length $T_{\text{FFT}} = 4$, (a) without noise correction (theoretical prediction and results from one simulation), (b) with noise correction (average over five simulations). Note the expanded scale in (b) showing drastic error reduction achieved by the noise reduction procedure.

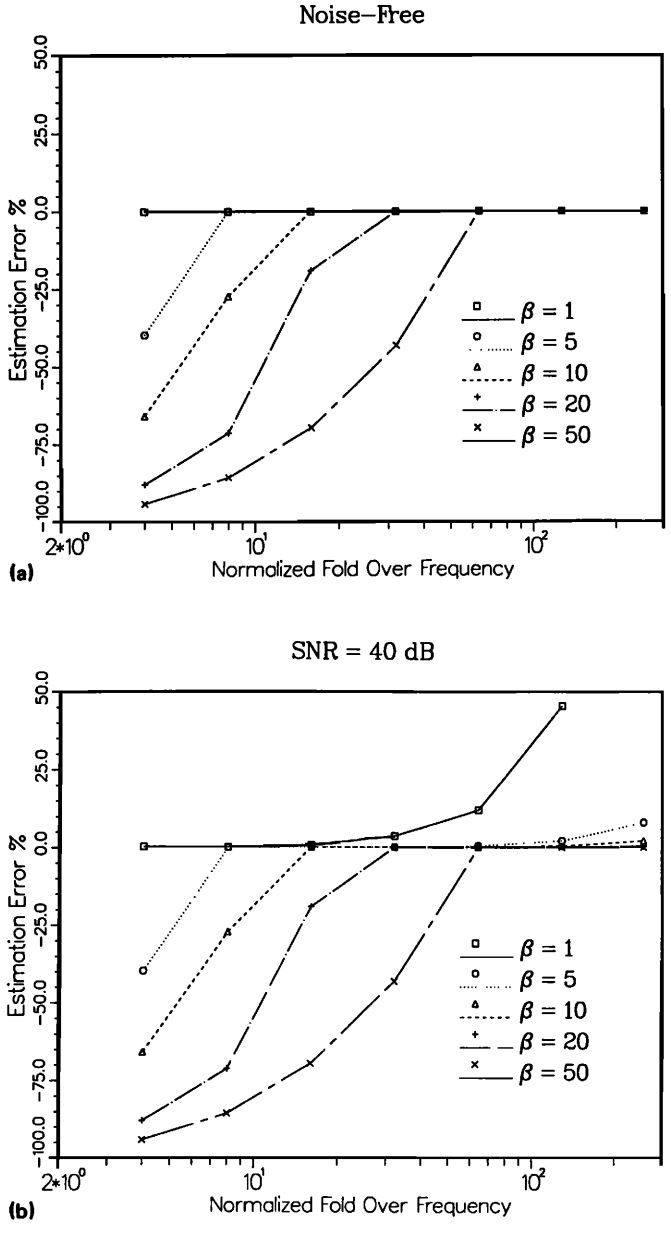

FIG. 6. Plot of estimation errors without noise correction against normalized fold-over frequency with $T_{\text{FFT}} = 4$, (a) noise-free, (b) signal-to-noise ratio SNR = 40 dB. As sampling frequency increases, underestimations originated from aliasing decrease in all cases. In (b), noise spectral spread causes large errors at high sampling rates since wideband white noise is employed in simulations.

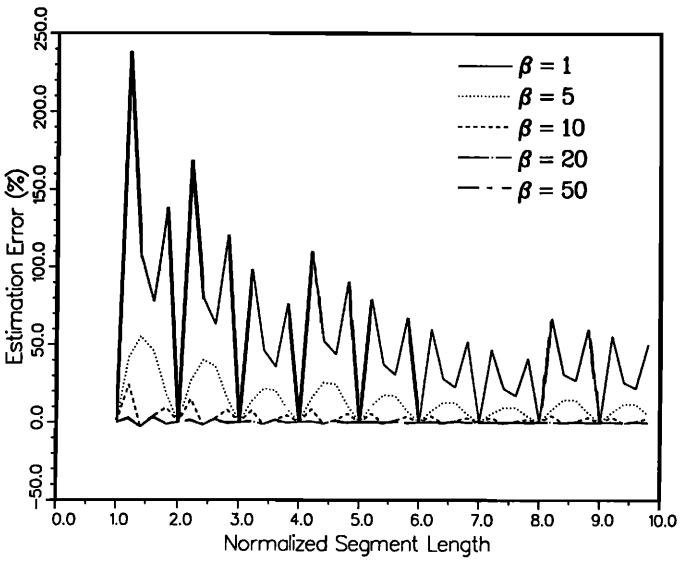

FIG. 7. Plot of noise-free estimation errors against normalized segment length $T_{\text{FFT}} = 4$. The finite-length effect produces overestimation. When the segment length is an integral multiple of vibration period, the estimation error drops to a minimum.

error resulting from the finite representation of the infinite spectrum. The normalized segment length (defined as segment length divided by the vibration period) is 4. Two sets of curves are shown in Fig. 5(a). The rapidly fluctuating one comes from a single simulation, while the smooth one is the theoretical prediction of the deviation of the estimation without any noise correction using Eq. (28). The simulation results agree with the theoretical prediction. These results show that the signal-to-noise ratio must be higher than about 30 dB to achieve acceptable accuracy of estimation unless noise correction procedure is performed.

From Eq. (25), the performance of the vibration estimator without noise correction will be degraded when the signal-to-noise ratio is low or the spectral spread of noise only is large compared to that of vibration only. When the parameter β is small, the spectral spread of the Bessel spectrum is narrow since the bandwidth (or spectral spread) is proportional to the parameter β from Eq. (23). In this case of low β, the spectral spread of noise is comparable or even larger than that of vibration only, thus the performance is highly degraded by the addition of the noise. When the parameter β is large as in wideband FM, the performance of the estimator is fairly good as long as β is still smaller than normalized fold-over frequency. The overestimation is due to the subtraction in Eq. (28).

Figure 5(b) is a plot of the estimation error with the noise correction algorithm. The vibration was removed to estimate the moments of the noise-only Doppler spectrum, and then the parameter β is estimated from the noisy signal by Eq. (28). Sampling conditions are the same as that in Fig. 5(a). Note the expanded vertical scale is Fig. 5(b). Obviously, dramatic error reduction is achieved through the noise correction procedure. The results of Fig. 5(b) are the average estimation errors over five simulations. The estimation errors are swinging back and forth around zero as the parameter β changes. This indicates that the estimator is unbiased. The maximum estimation error for poor signal-to-noise ratio at 0 dB is still within 4%. The estimation error of high β is much less than that of low β, as explained earlier.

B. Effects of sampling

The aliasing effect can be serious when the fold-over frequency or sampling frequency is not proper. Figure 6(a) shows the noise-free estimation error at normalized fold-over frequency expressed as a power of 2. The effect of the improper segmentation is minimal here since the normalized total length is four, as will be explained later. The estimation errors blow up at the point when the parameter β is larger than a threshold. This sampling criterion can be expressed as

$$f_s = 2f_{\text{fold}} \geqslant 2\beta_{\max} f_L, \tag{32}$$

where f_s is the sampling frequency, f_{fold} is the fold-over frequency, and f_L is the vibration frequency in Hz.

It is interesting to note that the aliasing always results in underestimation. The reason is that harmonics higher than fold-over frequency are folded back into lower frequency contents and the ω^2 or n^2 term associated with the higher harmonics in calculating the second moment is smaller than what it should be in the theoretical expressions (10), (14), and (23).

Figure 6(b) is the same simulation with 40 dB signal-to-noise ratio. Interestingly, as the fold-over frequency increases, the estimation errors increase as a second-order polynomial. This results from the property of the white Gaussian noise used in simulation. Since the spectral spread of a uniform spectrum is proportional to the second power of the bandwidth, as shown earlier in Eq. (31), the estimation error increases approximately as a second-order polynomial in normalized fold-over frequency when no filtering process is involved. Therefore, filtering should be taken if the sampling frequency is increased to avoid the aliasing error. In practice, filters can be designed to optimize the estimation according to the actual spectral moments of signal and noise.

Figure 7 is the plot of noise-free estimation error against normalized total sampling segment length T_{FFT}. To exclude the effect of aliasing error, the normalized fold-over frequency is set to 64. The estimation error is minimal whenever the normalized total sampling length is equal to an integer. The large error of nonintegral normalized total sampling length is due to the sharp discontinuity of the time domain signal from the inherent periodicity when FFT analysis is exploited without windowing. This indicates that windowing or synchronization is required in practical analysis. Note that the finite sampling length always causes overestimation. This happens as expected since the sharp discontinuity in time domain generates significant sidebands that can subsequently increase the spectral spread.

C. Effects of nonlinearity

If the vibration is not perfectly sinusoidal due to some medium or vibration source nonlinearity, the Doppler spec-

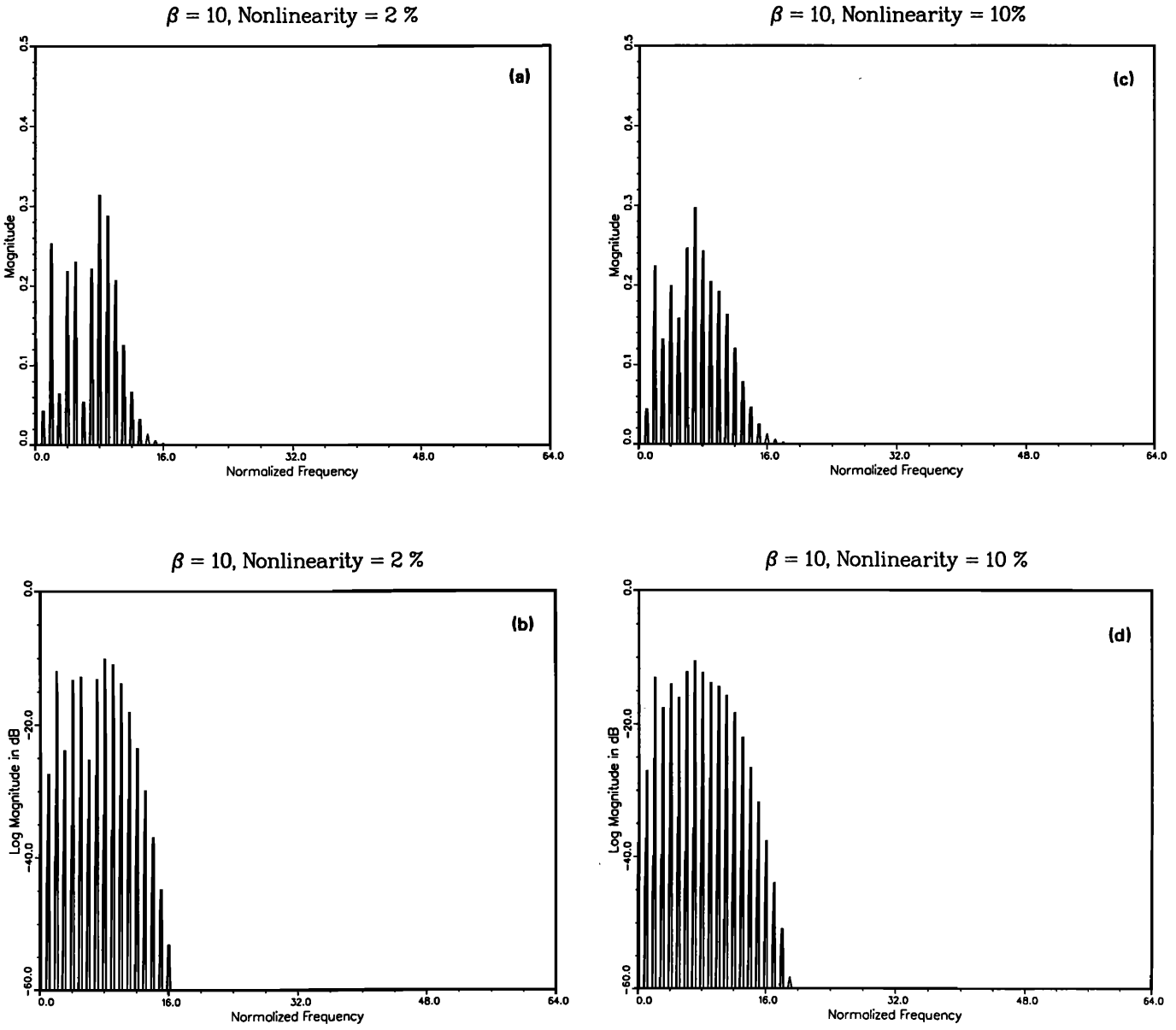

FIG. 8. Examples of noise-free Doppler spectrum for 2% and 10% nonlinearity with fundamental vibration amplitude $\beta = 10$, normalized fold-over frequency $f_{\text{fold}} = 64$ and normalized segment length $T_{\text{FFT}} = 4$. Note that the peaks of the spectra shift from the case of no nonlinearity (Fig. 1). The relative ratios of harmonics also vary as a function of nonlinearity, vibration amplitude, and fold-over frequency: (a) 2% nonlinearity, linear scale, (b) 2% nonlinearity, log scale, (c) 10% nonlinearity, linear scale, (d) 10% nonlinearity, log scale.

tral shape will deviate from the one parameter Bessel spectrum. Assuming the vibration is periodic and can therefore be represented by a Fourier series, both the ratio of harmonics and the spectral spread will be different from that of a pure sinusoidal vibration. Assuming that only the fundamental and second harmonics are significant in the vibration, the returned signal now can be written as

$$s_r(t) = A\cos[\omega_0 t + \beta\sin(\omega_L t + \varphi_1) + \beta_2\sin(2\omega_L t + \varphi_2)], \tag{33}$$

where β and β_2 are the modulation indices of the fundamental and second harmonics of the vibration, respectively.

An expression for the Fourier series expansion of the above signal can be obtained from the analysis of multitone FM[3] with slight modification as follows:

$$s_r(t) = \sum_{m=-\infty}^{\infty}\sum_{n=-\infty}^{\infty} J_m(\beta)J_n(\beta_2) \times\cos[\omega_0 t + m(\omega_L t + \varphi_1) + n(2\omega_L t + \varphi_2)]. \tag{34}$$

The nonlinearity is defined as

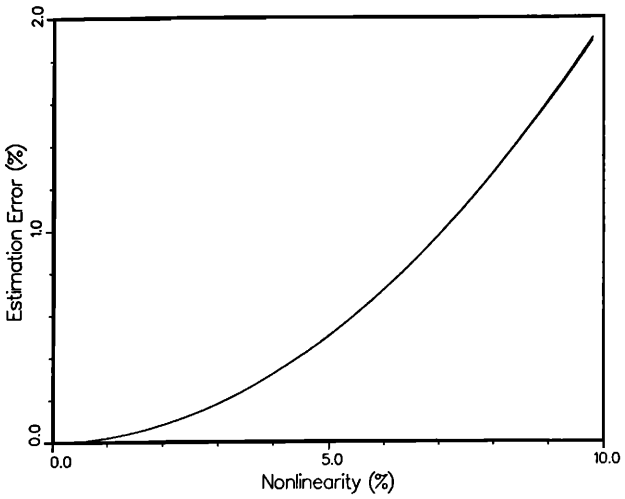

FIG. 9. Plot of noise-free estimation errors against nonlinearity. The errors are almost the same for all values of β from 0.1–50. The errors due to nonlinearity are less than 2% when nonlinearity is less than 10%.

$$\text{Nonlinearity} = N_2 \equiv (\beta_2/\beta) \times 100\%. \quad (35)$$

Figure 8 a–d shows the spectra of 2% and 10% nonlinearity for the case of $\beta = 10$. The spectral shapes and peaks are different from that of pure tone vibration (Fig. 1). Surprisingly, this does not affect the Doppler spectral spread much. Estimation for noise-free, small aliasing, and properly sampled signal has been performed as shown in Fig. 9. The results show that nonlinearity less than 10% contributes less than 2% estimation error. In comparison, all conventional estimators that utilize amplitude ratios would be dramatically affected by 10% nonlinearity. This can be appreciated by comparing the patterns of peak amplitudes in Fig. 1(c) against those in Fig. 8(c).

D. Combined effects

A case that is typical in "sonoelasticity imaging,"[7,12] with the following parameters, was performed to show the combined error:

$c_0 = 1.5 \times 10^5$ cm/s,

$f_0 = \omega_0/2\pi = 7.5$ MHz (i.e., $\lambda_0 = 0.2$ mm),

$\theta = 10°$,

$f_L = \omega_L/2\pi = 200$ Hz,

$\beta = 10$ (i.e., $\xi_m = 0.16$ mm, $v_m = 20.3$ cm/s),

SNR = 20 dB,

$f_{\text{fold}} = 12.8 f_L = 2560$ Hz (i.e., $f_s = 5120$ Hz),

$T_{\text{FFT}} = 10\, T_L = 50$ ms (i.e., $L_{\text{FFT}} = 256)l$,

$N_2 = 10\%$,

where T_{FFT} is the segment length for FFT analysis in ms, and L_{FFT} is the number of samples in T_{FFT}. The estimation error without noise correction is 3.39%, while the estimation is reduced to 1.97% after noise removal. Most of the error comes from the nonlinearity. If the nonlinearity is removed, estimator without noise correction gives accurate estimation within 0.01%, while the accuracy is increased to 0.0001% after noise correction.

If wideband white noise is added but no filtering process is used (same parameters, except $f_{\text{fold}} = 64 f_L$), then the estimation error for estimator without noise correction rises to 30.4%, while the error remains as small as 1.75% after noise correction. The large error is due to the large wideband-noise spectral spread as predicted in Eq. (31). This suggests that either noise correction or filtering is necessary for noise reduction when the sampling frequency is increased to reduce the aliasing error in practical implementation. If filtering is applied, the effects on signal spectral spread must be taken into account during the filter-design phase, since higher harmonics of the signals are removed as well. It should be noted that the performance of the estimator with noise correction can be improved by increasing sampling frequency without filtering.

III. CONCLUSION

We have analyzed the signal reflected from a sinusoidally vibrating object. An estimator of vibration amplitude based on the derived relation between Doppler spectral spread and vibration amplitude has been proposed. A noise correction algorithm is also proposed, which can improve the estimation accuracy dramatically. Simulations show good results within 4% error given signal-to-noise ratios ranging from 0–40 dB. Adequate sampling frequency, as given in the text, must be satisfied according to the expected maximum vibration amplitude. Proper filtering can reduce the spectral spread of noise and then reduce the estimation error. Windowing or synchronization is required in practical implementation to reduce the finite length effect. The proposed estimator survives through vibration nonlinearity less than 10%, whereas other known estimators that make use of the harmonic ratio of amplitudes do not tolerate slight nonlinearities. Overall, the proposed estimator is robust in the presence of noise compared to earlier estimators. The estimation can be obtained via simple calculations from the parameters in some existing Doppler instruments, especially those available in clinical Doppler ultrasound. To display a realtime vibration image, existing faster time domain Doppler spectral spread estimators (e.g., Refs. 13, 14) can be applied with modifications (e.g., changing scanning patterns and sampling frequency to reduce the effect of vibration phase) and/or synchronization (with low-frequency vibration) to display the vibration amplitude. The results should be relevant to echocardiology, sonoelasticity imaging, laser calibration of sound fields and vibration, and other radio, radar, and sonar applications.

ACKNOWLEDGMENTS

The support and encouragement of Dr. R. Gramiak and Dr. J. Holen are gratefully acknowledged. This work was supported by the Department of Electrical Engineering, University of Rochester.

[1]D. Censor, "Acoustical Doppler effect analysis—Is it a valid method?," J. Acoust. Soc. Am. **83**, 1223–1230 (1988).
[2]J. C. Piquette, A. L. Van Buren, and P. H. Rogers, "Censor's acoustical Doppler effect analysis—Is it a valid method?," J. Acoust. Soc. Am. **83**, 1681–1682 (1988).
[3]A. B. Carlson, *Communications Systems* (McGraw-Hill, New York, 1986), Chap. 8, pp. 221–227.
[4]J. Holen, R. C. Waag, and R. Gramiak, "Representations of rapidly oscillating structures on the Doppler display," Ultrasound Med. Biol. **11**, 267–272 (1985).
[5]K. J. Taylor, "Absolute measurement of acoustic particle velocity," J. Acoust. Soc. Am. **59**, 691–694 (1976).
[6]K. J. Taylor, "Absolute calibration of microphone by a laser Doppler," J. Acoust. Soc. Am. **70**, 939–945 (1981).
[7]R. M. Lerner, S. R. Huang, and K. J. Parker, "Sonoelasticity images derived from ultrasound signals in mechanically vibrated tissues," Ultrasound Med. Biol. **16**, 231–239 (1990).
[8]J. Jarzynski, D. Lee, J. Vignola, Y. H. Berthelot, and A. D. Pierce, "Fiber optics Doppler systems for remote sensing of fluid flow," in *Ocean Optics IX, Proceeding of SPIE Conference on Optics, Electro-Optics, and Sensors*, SPIE **925**, 250–254 (4–6 Apr. 1988).
[9]M. Cox and P. H. Rogers, "Automated noninvasive motion measurement of auditory organs in fish using ultrasound," J. Vib. Acoust. Str. Rel. Des. **109**, 55–59 (1987).
[10]Y. Yamakoshi, J. Sato, and T. Sato, "Ultrasonic imaging of internal vibration inside of soft tissue under forced vibration," IEEE Trans. Ultrason. Ferroelec. Freq. Control **UFFC-37**, 45–53 (1990).
[11]G. N. Watson, *Treatise on the Theory of Bessel Functions* (MacMillan, New York, 1945), Chap. 2, pp. 14–15, 31.
[12]R. M. Lerner, K. J. Parker, J. Holen, R. Gramiak, and R. C. Waag, "Sono-elasticity: Medical elasticity images derived from ultrasound signals in mechanically vibrated targets," Acous. Imag. **16**, 317–327 (1988).
[13]C. Kasai, K. Namekawa, A. Koyano, and R. Omoto, "Real-time two-dimensional blood flow imaging using an autocorrelation technique," IEEE Trans. Sonics Ultrason. **SU-32**, 458–463 (1985).
[14]K. Kristoffersen, "Time-domain estimation of the center frequency and spread of Doppler spectra in diagnostic ultrasound," IEEE Trans. Ultrason. Ferroelec. Freq. Control **UFFC-35**, 484–497 (1988).